Counterion Condensation on Flexible Polyelectrolytes: Dependence on Ionic Strength and Chain Concentration

H. Schiessel†

Materials Research Laboratory, University of California, Santa Barbara, California 93106-5130

Received January 13, 1999; Revised Manuscript Received June 10, 1999

ABSTRACT: We give a simple scaling picture for dilute and semidilute solutions of flexible polyelectrolytes including counterion condensation. It is shown that below a critical temperature a fraction of the counterions condenses on the chain. This leads to a renormalization of the total charge of the macroions as well as to a condensation-induced intrachain attraction resulting in a shrinkage of the chain. The paper extends the scaling picture of Schiessel and Pincus [*Macromolecules* **1998**, *31*, 7953] for dilute solutions without extra salt to higher ionic strengths and higher chain concentrations. The diagram of states for the different cases is presented.

1. Introduction

Scaling approaches to polyelectrolytes mostly focus on the case when the interaction of the macroions with the oppositely charged counterions can be neglected.[1−3] However, many synthetic and biological macroions (sulfonated polystyrene (PSS), DNA, ...) show strong electrostatic interactions between the chains and its counterions, and many numerical studies were devoted to this regime.[4−6] Manning condensation, first developed for the case of a single, infinitely long, charged, rigid rod,[7] is basic to the understanding of these systems: Counterions condense on the rod so long as the electrostatic attraction with the rod overwhelmes their translational entropy. The rigid rod picture can describe the behavior of chains with a long bare persistence length l_P, like DNA ($l_P \approx 500$ Å), but is not suitable for intrinsically flexible chains such as PSS ($l_P \approx 10$ Å). A scaling theory for this case is therefore desireable.

In ref 8 Schiessel and Pincus provided a scaling picture in terms of thermal blobs, focusing on the case of a dilute solution of macroions and no addional salt. It was shown that, with an increasing strength of the electrostatic interaction, counterion condensation sets in and chains begin to shrink. This contradicts single chain theories that predict a stretching of the chain with increasing strength of the interaction,[1−3] a picture that is only valid below the counterion-condensation threshold.

There are several theoretical approaches as well as computer simulations in which this effect is discussed. González-Mozuelos and Olvera de la Cruz[9] showed by minimizing the free energy of such a system that the macroions are stretched at higher temperatures and collapsed at low temperatures. Using a similar approach Brilliantov et al.[10] predicted numerically a first-order transition to a collapsed state at lower temperatures. The nonmonotonic dependence of the chain size on the strength of the electrostatic interaction was also found in MD-simulation of dilute solutions of highly charged chains with monovalent counterions by Stevens and Kremer[4] as well as by Winkler et al.[5] Most importantly, it is experimentally known that highly charged polyelectrolytes precipitate when one adds salt.[11] Furthermore, we note that counterion condensation may even induce a collapse of stiff polyelectrolytes, as it was recently shown theoretically.[12]

The present paper studies the behavior of polyelectrolyte solutions at different ionic strengths and different chain concentrations. In the following section, we review the case of a dilute solution of chains without added salt, as was considered in ref 8. Dilute solutions with a higher salinity are discussed in section 3. Section 4 is devoted to the case of entangled chains (semidilute solutions). Finally, we give a conclusion in section 5.

2. Dilute Solution without Salt

In this section, we briefly review the phase diagram of dilute solutions of perfectly flexible polyelectrolytes in the absence of excess ions (no added salt) as was presented in ref 8; for a more detailed discussion, we refer the reader to this reference. We consider chains consisting of N monomers ($N \gg 1$) of size b at a monomer concentration c far below the overlap threshold. The fraction of charged monomers is denoted by $f \leq 1$ so that the total charge per chain is $Z = fN$ (in units of the electronic charge e). Electroneutrality requires a finite concentration cf of counterions (we assume here monovalent ions carrying the charge $-e$). The phase diagram of this system as a function of solvent quality and temperature is shown in Figure 1; the different scaling relations are given in Table 1. We study first the behavior of the chains in a Θ solvent where the excluded volume v of the monomers vanishes, $v = 0$, starting from high temperatures and discussing the different states of the chain that occur with decreasing temperature. Following the same procedure, we will review then the cases where the solvent is good, $v > 0$, and poor, $v < 0$.

Θ Solvent, High-Temperature Limit (Regime 1 in Figure 1). At very high temperatures the electrostatic energy of the chain, $e^2Z^2/\epsilon L$ (ϵ, dielectric constant of the solvent; L, chain size), is smaller than the thermal energy T (temperature in units of the Boltzmann constant k_B) and the chain assumes Gaussian chain statistics, $L \simeq bN^{1/2}$. Introducing the Bjerrum length $l_B = e^2/\epsilon T$, we can rewrite the condition for the high-T limit as $l_B^{-1} > f^2N^{3/2}/b$.

† Present address: Department of Physics and Department of Chemistry and Biochemistry, University of California, Los Angeles, CA 90095.

10.1021/ma990051k CCC: $18.00
Published on Web 07/30/1999

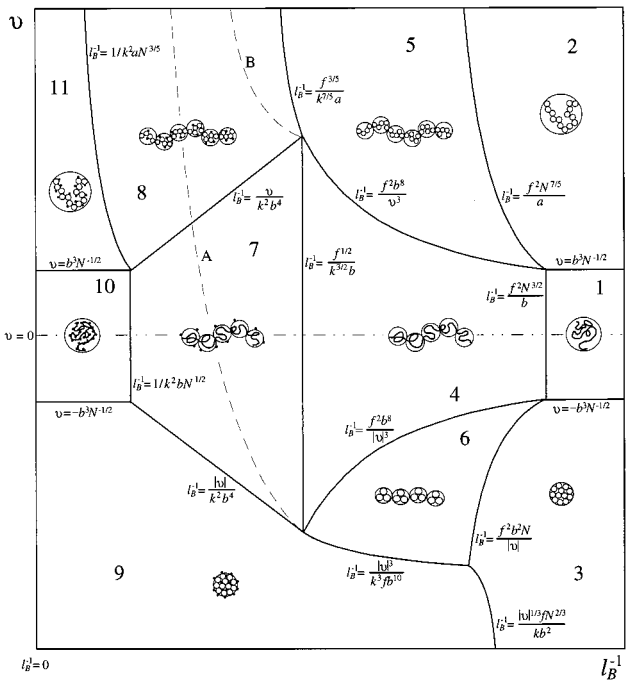

Figure 1. Phase diagram of a dilute solution of polyelectrolytes as a function of the solvent quality and the inverse Bjerrum length $l_B^{-1} \simeq \epsilon T/e^2$ (as presented in ref 8). For each regime the typical conformation of the macroion is depicted using the concept of blobs. The different length scales are summarized in Table 1. The dashed−dotted line $\upsilon = 0$ corresponds to a Θ solvent, $\upsilon > 0$ to a good solvent, and $\upsilon < 0$ to a poor solvent. The expressions for the scaling boundaries between the different regimes are given. This simple scaling theory does not account for fluctuation-induced electrostatic interactions that leads effectively to poorer solvent conditions in the case of condensed counterions (represented by the black dots). Lines A and B show qualitatively the actual phase boundaries between the regimes 7, 8, and 9 when one accounts for this effect (see text).

Θ Solvent, Stretched Chains without Counterion Condensation (Regime 4 in Figure 1). For smaller values of l_B^{-1} the repulsion between the monomers comes into play. The chain conformation is determined by the competition between the chain entropy and the electrostatic repulsion of the charged monomers. For large length scales, electrostatics dominates and leads to a rodlike shape, while for small scales entropy dictates Gaussian statistics. The resulting blob picture[1,3] consists of a string of electrostatic blobs of size ξ_{el} with g_{el} monomers. ξ_{el} and g_{el} can be determined from the condition that the electrostatic energy per blob is of the order T, i.e., $(fg_{el})^2 l_B/\xi_{el} \simeq 1$. Each blob obeys Gaussian chain statistics, i.e., $\xi_{el} \simeq bg_{el}^{1/2}$. Thus, $\xi_{el} \simeq b^{4/3}/l_B^{1/3}f^{2/3}$ and the total length $L \simeq (N/g_{el})\xi_{el}$ of the chain follows:[1,3]

$$L \simeq f^{2/3}b^{2/3}l_B^{1/3}N \qquad (1)$$

Θ Solvent, Stretched Chains with Counterion Condensation (Regime 7 in Figure 1). The picture described above breaks down at lower temperatures (smaller l_B^{-1}) when the electrostatic interaction $-e^2Z/\epsilon L$ between a counterion and a nearby chain[13] exceeds its translational entropy $-T\ln(\phi)$ (ϕ denotes the volume fraction of the counterions of volume v_c, i.e. $\phi \simeq cv_cf$). We treat the $\ln(\phi)$ term as a constant, $\ln(\phi) = -k$. For $l_B^{-1} < f^{1/2}/k^{3/2}b$, a fraction of the counterions will condense on the macroion and effectively reduce the total charge to a value $\tilde{Z} \simeq kL/l_B < Z$.[14,15] To describe a macroion with condensed counterions one can use again the blob picture, now with an effective charge fraction $\tilde{f} = \tilde{Z}/N$. The blob parameters ξ_{el} and g_{el} as well as $\tilde{f}$ are determined by the following conditions: $(\tilde{f}g_{el})^2 l_B/\xi_{el} \simeq 1$, $\xi_{el} \simeq bg_{el}^{1/2}$, and $\tilde{f} \simeq kL/l_BN \simeq k\xi_{el}/l_Bg_{el}$. One finds $\xi_{el} \simeq l_B/k^2$ and[8]

$$L \simeq \frac{k^2b^2N}{l_B} \qquad (2)$$

Equation 2 shows that the chain begins to shrink while the blobs grow with decreasing temperature as soon as counterion condensation sets in, an effect that follows from the decrease of the effective charge fraction. At very low temperatures, $l_B^{-1} < 1/k^2bN^{1/2}$, $\tilde{Z}$ is so small that the chain conformation is again governed by the configurational entropy, $L \simeq bN^{1/2}$ (regime 10 in Figure 1). We thus find a nonmonotonic dependence of the size of the polyelectrolyte on l_B. This agrees with computer simulations of dilute solutions of flexible polyelectrolyte chains[4,5] where the typical size of the chains are monitored as a function of l_B. The chains show clearly a shrinking as soon as counterion condensation sets in. They shrink, however, to a collapsed state with $L \propto N^{1/3}$ that is smaller than the high-T limit. This effect follows from the fluctuation-induced electrostatic attraction between monomers induced by the condensed counterions that effectively change the solvent quality as discussed at the end of this section.

Good Solvent (Regimes 2, 5, 8, and 11 in Figure 1). At high temperatures the electrostatic interaction can be neglected and the chain is swollen due to excluded volume effects.[16] The chain constitutes a self-avoiding walk of ideal thermal blobs of size $\xi_T \simeq b^4/\upsilon$. Thus, $L \simeq aN^{3/5}$ with $a = (\upsilon b^2)^{1/5}$. When $\upsilon < b^3N^{-1/2}$, one has $\xi_T > bN^{1/2}$ and the whole chain obeys Gaussian statistics, regime 1 in Figure 1. The chain begins to stretch when $l_B^{-1} < f^2N^{7/5}/a$ and can be described as a linear string of swollen electrostatic blobs (diameter $\xi_{el} \simeq a^{10/7}/l_B^{3/7}f^{6/7}$) of length[2,3]

$$L \simeq f^{4/7}a^{5/7}l_B^{2/7}N \qquad (3)$$

Regime 5 is present as long as $\xi_{el} > \xi_T$, i.e., as long as $l_B^{-1} > f^2b^8/\upsilon^3$. For smaller values of l_B^{-1} each electrostatic blob obeys ideal chain statistics; i.e., one enters regimes 4 and 7. At $l_B^{-1} \simeq \upsilon/k^2b^4$ the short-length repulsion leads again to a swelling of the blobs, regime 8. One finds $\xi_{el} \simeq l_B/k^2$ (as in the Θ-case) and[8]

$$L \simeq \frac{k^{4/3}a^{5/3}N}{l_B^{2/3}} \qquad (4)$$

The chain shrinks with decreasing l_B^{-1} and reaches at $l_B^{-1} \simeq 1/k^2aN^{3/5}$ the unperturbed value $L \simeq aN^{3/5}$ (regime 11).

Poor Solvent (Regimes 3, 6, and 9 in Figure 1). For the case of a macroion in an athermal poor solvent with $\upsilon < 0$, one encounters—similar to the good solvent case— thermal blobs of size $\xi_T \simeq b^4/|\upsilon|$. The short-range attraction induces the structure of a molten globule with densely packed thermal blobs of size $L \simeq b^2N^{1/3}/|\upsilon|^{1/3}$. Missing neighboring blobs lead to a surface tension $\gamma \simeq T/\xi_T^2$; the surface energy of the globule is then γL^2. This picture remains valid as long as the surface energy is larger than the electrostatic energy $(efN)^2/\epsilon L$, i.e., as

Table 1. Characteristic Length Scales in Solutions of Polyelectrolytes: Electrostatic Blob Size ξ_{el}, Mesh Size ξ_m (for the Case of Overlapping Chains), Electrostatic Persistence Length l_e, and Total Size L of a Single Chain[a]

regime	ξ_{el}	ξ_m	l_e	L
1/10				$bN^{1/2}$
2/11				$aN^{3/5}$
3/9				$b^2N^{1/3}/\lvert v\rvert^{1/3}$
4	$b^{4/3}/l_B^{1/3}f^{2/3}$			$f^{2/3}b^{2/3}l_B^{1/3}N$
4_s	$b^{4/3}/l_B^{1/3}f^{2/3}$		$f^{2/3}/b^{4/3}l_B^{2/3}c_s$	$f^{8/15}b^{2/15}N^{3/5}/l_B^{1/30}\ c_s^{3/10}$
4_o	$b^{4/3}/l_B^{1/3}f^{2/3}$	$1/c^{1/2}f^{1/3}b^{1/3}l_B^{1/6}$	$1/c^{1/2}f^{1/3}b^{1/3}l_B^{1/6}$	$f^{1/6}b^{1/6}l_B^{1/12}N^{1/2}/c^{1/4}$
5	$a^{10/7}/l_B^{3/7}f^{6/7}$			$f^{4/7}a^{5/7}l_B^{2/7}N$
5_s	$a^{10/7}/l_B^{3/7}f^{6/7}$		$f^{6/7}/c_sl_B^{4/7}a^{10/7}$	$f^{18/35}a^{1/7}N^{3/5}/c_s^{3/10}\ l_B^{3/70}$
5_o	$a^{10/7}/l_B^{3/7}f^{6/7}$	$1/c^{1/2}f^{2/7}a^{5/14}l_B^{1/7}$	$1/c^{1/2}f^{2/7}a^{5/14}l_B^{1/7}$	$f^{1/7}a^{5/28}l_B^{1/14}N^{1/2}/c^{1/4}$
6	$b^{4/3}/l_B^{1/3}f^{2/3}$			$f^{4/3}b^{10/3}l_B^{2/3}N/\lvert v\rvert$
6_s	$b^{4/3}/l_B^{1/3}f^{2/3}$		$f^{2/3}/c_sl_B^{2/3}b^{4/3}$	$f^{14/15}b^{26/15}l_B^{1/6}N^{3/5}/c_s^{3/10}\lvert v\rvert^{3/5}$
6_o	$b^{4/3}/l_B^{1/3}f^{2/3}$	$\lvert v\rvert^{1/2}/c^{1/2}f^{2/3}b^{5/3}l_B^{1/3}$	$\lvert v\rvert^{1/2}/c^{1/2}f^{2/3}b^{5/3}l_B^{1/3}$	$f^{1/3}b^{5/6}l_B^{1/6}N^{1/2}/\lvert v\rvert^{1/4}c^{1/4}$
7	l_B/k^2			k^2b^2N/l_B
7_s	l_B/k'^2		$k'^2/c_sl_B^2$	$k'^{8/5}b^{6/5}N^{3/5}/l_B^{11/10}\ c_s^{3/10}$
7_o	l_B/k^2	$l_B^{1/2}/kc^{1/2}b$	$l_B^{1/2}/kc^{1/2}b$	$k^{1/2}b^{1/2}N^{1/2}/c^{1/4}l_B^{1/4}$
8	l_B/k^2			$k^{4/3}a^{5/3}N/l_B^{2/3}$
8_s	l_B/k'^2		$k'^2/c_sl_B^2$	$k'^{6/5}aN^{3/5}/c_s^{3/10}\ l_B^{9/10}$
8_o	l_B/k^2	$l_B^{1/3}/k^{2/3}c^{1/2}a^{5/6}$	$l_B^{1/3}/k^{2/3}c^{1/2}a^{5/6}$	$k^{1/3}a^{5/12}N^{1/2}/c^{1/4}l_B^{1/6}$

[a] The different regimes 1 to 11 are depicted in the phase diagrams, Figures 1−3. The indices denote modifications of the salt-free dilute case by screening, s, and chain overlap, o.

long as $l_B^{-1} \simeq f^2b^2N/|v|$. At this value a Rayleigh-type instability[17] occurs, the globule breaks up and the chain stretches out. A simple description of this state using the concept of electrostatic blobs goes back to Khokhlov.[18] The size of the blobs is determined by the competition between electrostatic repulsion and surface tension, i.e., $(fg_{el})^2l_B/\xi_{el} \simeq \xi_{el}^2/\xi_T^2$. Together with poor solvent statistics $\xi_{el} \simeq b^2g_{el}^{1/3}/|v|^{1/3}$ one finds $\xi_{el} \simeq b^{4/3}/l_B^{1/3}f^{2/3}$ and

$$L \simeq \frac{f^{4/3}b^{10/3}l_B^{2/3}N}{|v|} \tag{5}$$

By decreasing l_B^{-1} one enters at $l_B^{-1} \simeq f^2b^8/|v|$ regime 4 where the electrostatic blobs obey Gaussian statistics and at $l_B^{-1} = f^{1/2}/k^{3/2}b$ regime 7 (ideal blobs with condensed counterions). In regime 7 one has $\xi_{el} \simeq l_B/k^2$. At $l_B^{-1} \simeq |v|/k^2b^4$ where $\xi_{el} \simeq \xi_T$ the statistics within the electrostatic blobs begins to change. For smaller values of l_B^{-1}, we may tentatively use again the picture of collapsed electrostatic blobs, now with condensed counterions. By equating the electrostatic energy and the surface tension, we find $\xi_{el} \simeq k^2b^8/v^2l_B$ and $L \simeq |v|^3l_B^2N/k^4b^{10}$. This argument leads to the counterintuitive prediction that the chain stretches with decreasing l_B^{-1}. This result is not consistent: starting at the crossover $l_B^{-1} \simeq |v|/k^2b^4$ ($\xi_{el} \simeq \xi_T$) and decreasing l_B^{-1}, the above given argument predicts $\xi_{el} \propto l_B^{-1}$ and thus $\xi_{el} < \xi_T$ as soon as the chain begins to stretch; i.e., the electrostatic blobs do not obey poor solvent statistics as assumed in this picture. Indeed, the more detailed study in ref 8 suggests that in regime 9 the globular state with $L \simeq b^2N^{1/3}/|v|^{1/3}$ is the state of lowest free energy. The transition from regime 7 to 9 (and also from regime 6 to 9) occurs as a first-order collapse enhanced by an avalanche-type counterion condensation as already suggested by Khokhlov.[18] A similar mechanism for polyelectrolytes with an annealed charge distribution in a poor solvent was discussed by Raphael and Joanny.[19] By crossing from regime 7 to 9 the renormalized charge decreases rapidly from $\tilde{Z} = k^{-1}(v/b^3)^2N$ to the much lower value $\tilde{Z} \simeq k^{-1}(|v|/b^3)^{2/3}N^{1/3}$. In our considerations of the poor solvent case we assumed that the chain assumes a cylindrical shape of diameter ξ_{el}. Dobrynin, Rubinstein and Obukhov showed in ref 20 that the macroion can lower its free energy further by stretching into a necklace structure with beads of size ξ_{el} connected by strings of diameter ξ_T. This only modifies the chain structure within regime 6. The phase boundaries of this regime are not changed, and it is also predicted that the necklace collapses as soon as counterion condensation sets in.[21] Note that recent computer simulations report necklace chains with condensed counterions,[6] a result that is not consistent with the scaling picture. This may be explained by the strong hydrophobicity and/or the short chain lengths ($N = 94$, $f = {}^1/_3$) used in the simulations; simulations with longer chains and smaller v are in progress.[23]

Effect of the Counterion-Induced Attraction. Up to now we assumed that the only effect of counterion condensation is the renormalization of the total charge. However, as soon as there are condensed counterions on a macroion they induce attractions between monomers. In ref 8 we accounted for this effect by shifting to poorer solvent conditions, i.e., $v' \simeq v - \Delta v$. Δv is calculated by assuming that condensed counterions form dipoles with oppositely charged monomers. Accounting for the angle-averaged potentials between the dipoles as well as between dipoles and monopols (monomers with no compensating counterion) one finds[8]

$$v' \simeq v - (f - \tilde{f})fl_B^2b \tag{6}$$

We note that eq 6 may have a more complicated form that depends on the ratio of different microscopic length scales as discussed in ref 8. Here we assume the simple case of the presence of only a single microscopic length scale, namely the monomer size b. Assume now that the chains are in regime 7 near the line $l_B^{-1} = f^{1/2}/k^{3/2}b$, i.e., when only a small amount of counterions is condensed. Then $f - \tilde{f} \simeq 0$ and $v' \simeq v$. By lowering l_B^{-1}, more and more counterions condense and therefore v' decreases. Finally, the attraction between the monomers becomes so strong that the thermal blobs $\xi_T \simeq b^4/|v'|$ becomes of the same order as the electrostatic blob size $\xi_{el} \simeq l_B/k^2$. Equating ξ_T and ξ_{el} one finds

$$-v \simeq \frac{b^4k^2}{l_B} + fk^3b^3 - f^2bl_B^2 \tag{7}$$

The corresponding line is depicted in the phase diagram,

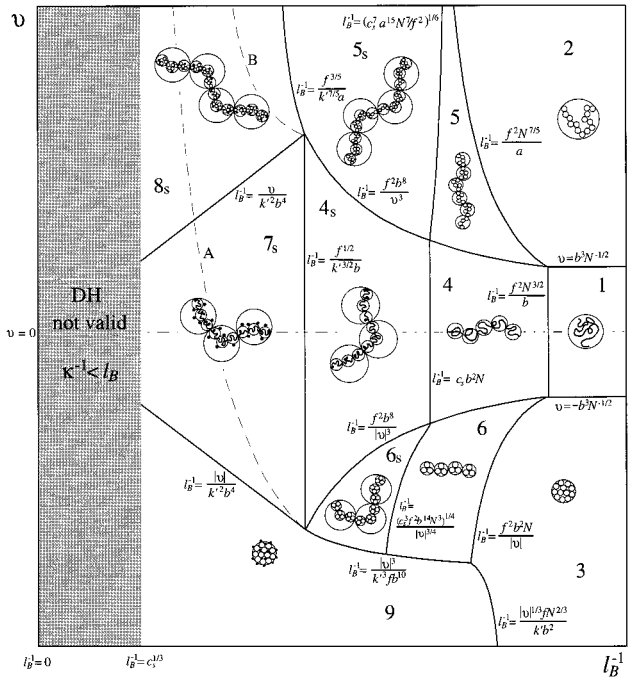

Figure 2. Diagram of states of a dilute solution of polyelectrolytes at higher ionic strength as a function of v and $l_B^{-1} \simeq \epsilon T/e^2$. See also Table 1. For $l_B^{-1} < c_s^{1/3}$ saturation effects come into play (shaded area).

Figure 1, as the dashed line A. The line starts at the point where regimes 4, 6, 7, and 9 come together. The more detailed study in ref 8 shows that the exact shape of this line (for instance, the l_B^{-1} value where it crosses the $v = 0$ line) depends on microscopic properties. In any case, even for more refined approaches we expect that the qualitative shape of line A is captured by eq 7. When one crosses line A, the poor solvent statistics becomes important and, as discussed above, the chain collapses in a first-order type fashion into a globular state with $L \propto N^{1/3}$. A discussion of the collapsed state is given in ref 8. Note further that regime 8 becomes strongly modified. One has swollen electrostatic blobs in the small band between the line $l_B^{-1} = f^{3/5}/k^{7/5}a$ and line B. At this line the sizes $\xi_{el} \simeq l_B/k^2$ and $\xi_T \simeq b^4/|v'|$ become comparable which leads to $v \simeq b^4k^2/l_B - fk^3b^3 + f^2bl_B^2$.

3. Dilute Solution at Higher Ionic Strength

Here we study the effect of adding salt to a dilute solution of polyelectrolytes. In this case the electrostatic interaction between the charged monomers becomes short-ranged with a Debye screening length $\kappa^{-1} \simeq c_s^{-1/2} l_B^{-1/2}$ (where c_s denotes the concentration of salt). Before we calculate the diagram of states, Figure 2, a word of caution has to be added. It is clear that in the case $\kappa^{-1} < L$ screening between monomers that are farer apart in space than κ^{-1} comes into play; it is therefore tempting to assume that in this case the chain behaves as a wormlike chain of electrostatic blobs with an electrostatic persistence length $l_e \simeq \kappa^{-1}$. This is indeed the assumption of the earlier works,[2,3] and it is supported by variational approaches.[3] l_e may, however, be much larger than κ^{-1}, a fact that is well-known for stiff polyelectrolytes with a sufficiently long bare persistence length l_P so that $l_P \gg b^2/(f^2l_B)$ (Odijk−Skolnick−Fixman (OSF) theory, see refs 3, 24, and 25). In this case it follows from a perturbation calculation that the chain has an effective persistence length $l_P + l_e$ with l_e given by $l_e = f^2l_B/4b^2\kappa^2$ (see remark 26 for a simple "scaling" derivation of this result). Khokhlov and Katchaturian[28] (KK) have proposed that this effects also carries over to flexible chains where the electrostatic blobs play the role of the monomers of a coarse-grained wormlike chain. Thus, the values of b and f^2l_B that occur in the OSF-theory have to be replaced by the electrostatic blob size ξ_{el} and by $f^2g_{el}^2l_B$. This leads to the following electrostatic persistence length:

$$l_e \simeq f^2g_{el}^2l_B/\xi_{el}^2\kappa^2 = 1/\kappa^2\xi_{el} \tag{8}$$

Even though computer simulations seem to indicate a more involved picture,[32] very recent careful theoretical studies strongly support this picture (cf. refs 29−31). We will therefore employ the KK-procedure in this section. As in the previous section we will first study the case of a Θ solvent and discuss the behavior of the system with decreasing value of l_B^{-1}.

Θ Solvent, Higher Temperatures (Regime 1 and 4 in Figure 2). At sufficiently large values of l_B^{-1} the persistence length is larger than the chain size, $l_e > L$, and the screening is unimportant. As discussed in the previous section the chain size is then given by $L \simeq bN^{1/2}$ in regime 1 and by eq 1 in regime 4 (cf. Figure 2). In this regime one has $\xi_{el} \simeq b^{4/3}/l_B^{1/3}f^{2/3}$, which implies an electrostatic persistence length $l_e \simeq f^{2/3}l_B^{1/3}\kappa^{-2}/b^{4/3} \simeq f^{2/3}/b^{4/3}l_B^{2/3}c_s$. At $l_B^{-1} \simeq c_sb^2N$, one has $l_e \simeq L$ and screening comes into play.

Θ Solvent, Wormlike Chain without Counterion Condensation (Regime 4_s in Figure 2). In this regime the chain can be envisaged as a semiflexible chain of electrostatic blobs with a finite persistence length l_e. The electrostatic blobs are given by a local argument, namely the interplay of the (unscreened) electrostatic repulsion and the thermal fluctuation, and their size is therefore identical to that of regime 4, i.e., $\xi_{el} \simeq b^{4/3}/l_B^{1/3}f^{2/3}$. Thus, the electrostatic persistence length l_e is still given by $l_e \simeq f^{2/3}/b^{4/3}l_B^{2/3}c_s$. The global configuration of such a chain can be calculated as follows (similar to the argument given by Odijk and Houwaart in ref 33): Due to the screened electrostatic repulsion the chain behaves effectively as a rescaled flexible chain with highly anisotropic, e.g., cylindrical monomers of length l_e and diameter κ^{-1}. This leads to a second virial coefficient for the segment−segment interaction of the form $\tilde{v} \simeq l_e^2\kappa^{-1}$. One has $\tilde{N} \simeq L_c/l_e$ segments where L_c is the "contour" length of the chain given by eq 1. The size of the chain follows from $L \simeq (\tilde{v}l_e^2)^{1/5}\tilde{N}^{3/5} \simeq L_c^{3/5}/c_s^{3/10}\, l_B^{3/10}\, \xi_{el}^{1/5}$, which leads to

$$L \simeq \frac{f^{8/15}b^{2/15}N^{3/5}}{l_B^{1/30}\, c_s^{3/10}} \tag{9}$$

As expected, the chain shrinks with increasing salt concentration. We call this regime 4_s, the index s denoting screening.

Θ Solvent, Wormlike Chain with Counterion Condensation (Regime 7_s in Figure 2). Consider a counterion that is near to a macroion so that the shortest distance to the macroion is smaller than κ^{-1}. Due to screening the counterion can see only a part of the chain of length $\kappa^{-1} < l_e$. Therefore, the macroion acts as a charged rod of length κ^{-1}. The electrical interaction with the macroion is then given by $e^2Z_D/\epsilon\kappa^{-1}$ (up to logarithmic corrections[13]); Z_D denotes the number of

charges on the chain section of length κ^{-1}. Counterions will condense and renormalize Z_D to the value $\tilde{Z}_D \simeq k'\kappa^{-1}/l_B$; cf. the previous section. Here, $k' = -\ln(\phi) = -\ln(c_s v_c)$ depends logarithmically on the salt concentration. The charge fraction is now given by $\tilde{f} \simeq k'\kappa^{-1}/g_D l_B$, where g_D denotes the number of monomers of the chain section under consideration. This together with $(\tilde{f}g_{el})^2 l_B/\xi_{el} \simeq 1$, $\xi_{el} \simeq b g_{el}^{1/2}$ and $\kappa^{-1} \simeq (g_D/g_{el})\xi_{el}$ leads to $\xi_{el} \simeq l_B/k'^2$, i.e., to the same blob size as in the salt-free case (up to logarithmic corrections). Now using the KK-scheme (using $\tilde{f}$ instead of f) we find again an electrostatic persistence length l_e which is given by eq 8. Thus, $l_e \simeq k'^2/c_s l_B^2$. This leads to the chain size

$$L \simeq \frac{L_c^{3/5}}{c_s^{3/10} l_B^{3/10} \xi_{el}^{1/5}} \simeq \frac{k'^{8/5} b^{6/5} N^{3/5}}{l_B^{11/10} c_s^{3/10}} \qquad (10)$$

where L_c is given by eq 2.

Good Solvent (Regimes 2, 5, 5_s, and 8_s in Figure 2). At sufficiently high temperatures one has $l_e > L$ and the screening can be neglected; cf. regimes 2 and 5 in Figure 2. When $l_B^{-1} \simeq (c_s^7 a^{15} N^7/f^2)^{1/6}$ the size L of the stretched macroion (cf. eq 3) is of the order of the electrostatic persistence length $l_e \simeq f^{6/7}/c_s l_B^{4/7} a^{10/7}$. For smaller values the size is given by $L \simeq L_c^{3/5}/c_s^{3/10} l_B^{3/10} \xi_{el}^{1/5}$. Below the condensation threshold, regime 5_s, one finds from eq 3

$$L \simeq \frac{f^{18/35} a^{1/7} N^{3/5}}{c_s^{3/10} l_B^{3/70}} \qquad (11)$$

In the case of counterion condensation, regime 8_s, the chain length obeys

$$L \simeq \frac{k'^{6/5} a N^{3/5}}{c_s^{3/10} l_B^{9/10}} \qquad (12)$$

Regime 5_s and 8_s have been studied in an MD-simulation in ref 34 using an explicit treatment of the salt ions. Qualitative features such as the shrinkage of chains with increasing salt concentration are in accordance with the scaling picture but the explicit comparison of the scaling exponents is not possible since the chains are too short.

Poor Solvent (Regimes 3, 6, 6_s, and 9 in Figure 2). For high temperatures where screening is unimportant one has collapsed globules of size $L \simeq b^2 N^{1/3}/|v|^{1/3}$, regime 3 in Figure 2, and stretched chains of length L given by eq 5, regime 6. Screening comes into play when $l_e < L$ with $l_e \simeq f^{2/3}/c_s l_B^{2/3} b^{4/3}$ (same as in the Θ case), i.e. for $l_B^{-1} < (c_s^3 f^2 b^{14} N^3/|v|^3)^{1/4}$. Using again $L \simeq L_c^{3/5}/c_s^{3/10} l_B^{3/10} \xi_{el}^{1/5}$, where L_c is now given by eq 5, we find

$$L \simeq \frac{f^{14/15} b^{26/15} l_B^{1/6} N^{3/5}}{c_s^{3/10} |v|^{3/5}} \qquad (13)$$

In the poor solvent case with counterion condensation, regime 9, we may tentatively use the concept of electrostatic blobs with condensed ions. Again, as in the previous section, we end up with an inconsistency, since a stretching of the total length (here the contour length) is predicted. This indicates that the chain collapses in a first-order transition into the collapsed state of size $L \simeq b^2 N^{1/3}/|v|^{1/3}$. Figure 2 also depicts the lines A and B that follow from the counterion-induced shift of the phases toward poorer solvent conditions, as discussed at the end of the previous section. Line A is still given by eq 7 with k replaced by k'.

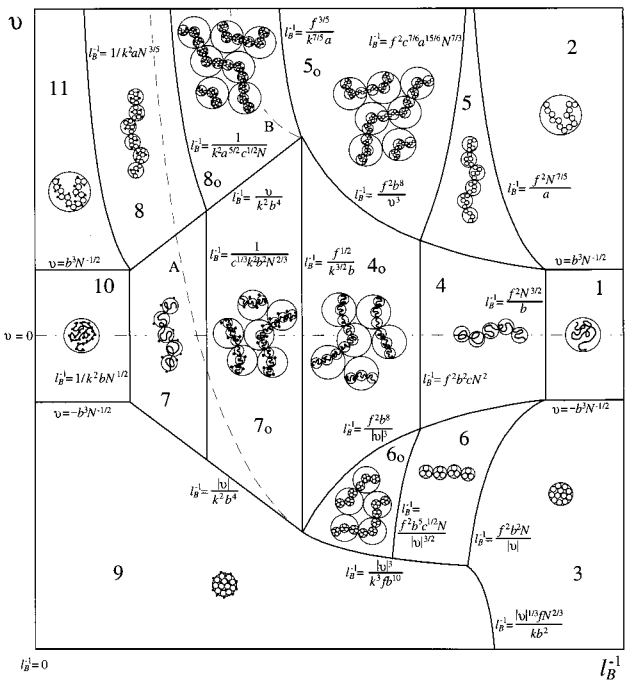

Figure 3. Phase diagram of a semidilute solution of macroions without extra salt as a function of v and $l_B^{-1} \simeq \epsilon T/e^2$. See also Table 1.

Finally, we note that the Debye−Hückel picture will only hold as the typical interaction between salt ions is smaller than T, i.e., as long as $l_B^{-1} > c_s^{1/3}$ or equivalently $\kappa^{-1} > l_B$. This condition also happens to coincide with the condition $\xi_{el} < \kappa^{-1}$ that has to be imposed on regime 7_s and 8_s. For $l_B^{-1} < c_s^{1/3}$, the system saturates; the resulting phase transition is beyond the scope of this paper.

4. Semidilute Solutions

Until now, we considered dilute solutions where the different chains are well separated from each other. In this section, we will focus on intermediate macroion concentrations where the chains are well separated at high temperatures but begin to overlap more and more with decreasing temperatures due to the stretching of the chains. We give a thorough discussion of the salt-free case (cf. Figure 3) and sketch the semidilute case at a higher salinity only briefly at the end of this section. We follow the lines of ref 1, where the scaling properties of semidilute solution of polyelectrolytes have been derived (without counterion condensation); see also refs 2 and 36.

Θ Solvent, below the Overlap Threshold at High Temperatures (Regimes 1 and 4 in Figure 3). Chains at high temperatures in dilute solutions form random walks with $L \simeq bN^{1/2}$ (cf. Section 2). If one increases the monomer concentration c, the chains will begin to overlap at $c = c^*$ where the overlap concentration is given by $c^* \simeq N/L^3 \simeq b^{-3}N^{-1/2}$. In the following, we assume that $c < c^*$; i.e., the concentration is so small that the Gaussian coils do not overlap (regime 1 in Figure 3). However, we assume that the concentration is high enough that the chains overlap considerably when they are in the strongly stretched state. In regime 4 where the size is given by $L \simeq f^{2/3} b^{2/3} l_B^{1/3} N$, cf. eq 1,

the chain stretches with decreasing l_B^{-1} which is accompanied by a lowering of $c^* \simeq N/L^3 \simeq 1/f^2b^2l_BN^2$. At $l_B^{-1} \simeq f^2b^2cN^2$ one reaches $c = c^*$, i.e., the chains begin to overlap.

Θ Solvent, Overlapping Chains without Condensed Counterions (Regime 4_o in Figure 3). Beyond the overlap threshold, $c > c^*$, the overlapping chains form a transient network with a typical mesh size ξ_m (the notation 4_o denotes regime 4 with overlapping chains). The scaling form of ξ_m follows from two requirements: (i) At the overlap threshold, $c = c^*$, ξ_m equals the chain size of noninterpenetrating chains, eq 1. (ii) For $c > c^*$, the mesh size is independent of the degree of polymerization N, $\xi_m \propto N^0$. This leads to the scaling form $\xi_m \simeq L(c^*/c)^{1/2}$. From this it follows that the mesh size obeys $\xi_m \simeq 1/c^{1/2}f^{1/3}b^{1/3}l_B^{1/6}$. Within the mesh size one finds, from the picture of electrostatic blobs, $\xi_m \simeq f^{2/3}b^{2/3}l_B^{1/3}g_m$ (cf. eq 1) where g_m denotes the number of monomers within the mesh size. It is generally believed that on larger length scales each chain will have many deflections that are induced by the presence of other chains; the distance between deflections will be of the order of the mesh size (see refs 3 and 35). Together with the Flory screening theorem,[16] this means that the configuration of a given chain is that of a random walk of step size ξ_m, i.e., $L \simeq \xi_m(N/g_m)^{1/2}$ which leads to[1]

$$L \simeq \frac{f^{1/6}b^{1/6}l_B^{1/12}N^{1/2}}{c^{1/4}} \tag{14}$$

In this argument, we implicitly assumed that the screening from the counterions can be neglected for length scales smaller than the mesh size, i.e. $\xi_m < \kappa^{-1} \simeq 1/c^{1/2}f^{1/2}l_B^{1/2}$. This translates into the condition $l_B^{-1} > f^{1/2}/b$, which coincides with the condition that the interaction between counterions and chains can be neglected, $l_B^{-1} > f^{1/2}/k^{3/2}b$. For smaller values of l_B^{-1}, one has counterion condensation.

Θ Solvent, Overlapping Chains with Condensed Counterions (Regime 7_o in Figure 3). For $l_B^{-1} < f^{1/2}/k^{3/2}b$, some counterions condense. From eq 2 we find the overlap threshold $c^* \simeq N/L^3 \simeq l_B^3/k^6b^6N^2$ and the mesh size $\xi_m \simeq L(c^*/c)^{1/2} \simeq l_B^{1/2}/c^{1/2}kb$. Using the picture of electrostatic blobs with condensed counterions, one finds, as in the dilute case (cf. sections 2 and 3), $\xi_{el} \simeq l_B/k^2$. From $\xi_m \simeq k^2b^2g_m/l_B$ (cf. eq 2) and $L \simeq \xi_m(N/g_m)^{1/2}$, one obtains

$$L \simeq \frac{k^{1/2}b^{1/2}N^{1/2}}{c^{1/4}l_B^{1/4}} \tag{15}$$

It is important to check if this argument is consistent. The Debye screening length that follows from the presence of free counterions is given by $\kappa^{-1} \simeq 1/c^{1/2}\tilde{f}^{1/2}l_B^{1/2}$ where the fraction of free counterions is given by $\tilde{f} \simeq k\xi_m/g_ml_B \simeq k^3b^2/l_B^2$. This leads to $\kappa^{-1} \simeq l_B^{1/2}/c^{1/2}k^{3/2}b$, which is of the same order as the mesh size; i.e. counterion condensation pins the screening length to the mesh size. It is therefore consistent to assume that the persistence length of the chains is given by ξ_m.

Θ Solvent, below the Overlap Threshold at Low Temperatures (Regimes 7 and 10 in Figure 3). In regime 7_o the chains shrinks with a decreasing value of l_B^{-1} as $L \propto l_B^{-1/4}$, cf. eq 15. At $l_B^{-1} \simeq 1/c^{1/3}k^2b^2N^{2/3}$ one leaves the overlap regime again and reenters a dilute regime, namely regime 7 where the chain size is given by eq 2, followed by regime 10.

Good Solvent, below the Overlap Threshold at High Temperatures (Regime 2 and 5 in Figure 3). At high temperatures the chains do not overlap so that one has isolated swollen coils with $L \simeq aN^{3/5}$ (regime 2) and stretched configurations with L given by eq 3 (regime 5). The chains begin to overlap at $l_B^{-1} \simeq f^2c^{7/6}a^{15/6}N^{7/3}$.

Good Solvent, Overlapping Chains without Condensed Counterions (Regime 5_o in Figure 3). When $l_B^{-1} < f^2c^{7/6}a^{15/6}N^{7/3}$ the chains overlap. The overlap concentration $c^* \simeq 1/f^{12/7}a^{15/7}l_B^{6/7}N^2$ predicts for the mesh size $\xi_m \simeq L(c^*/c)^{1/2} \simeq 1/c^{1/2}f^{2/7}a^{5/14}l_B^{1/7}$. The number of monomers g_m within this correlation length is given by the relation $\xi_m \simeq f^{4/7}a^{5/7}l_B^{2/7}g_m$; cf. eq 3. Excluded volume and electrostatics is screened at length scales larger than ξ_m so that $L \simeq \xi_m(N/g_m)^{1/2}$. This leads to[2,36]

$$L \simeq \frac{f^{1/7}(vb^2)^{1/28}l_B^{1/14}N^{1/2}}{c^{1/4}} \tag{16}$$

Note the weak dependencies of L on v and l_B.

Good Solvent, Overlapping Chains with Condensed Counterions (Regime 8_o in Figure 3). At $l_B^{-1} \simeq f^{1/2}/k^{3/2}b$, counterion condensation sets in. From eq 4, one finds for the overlap threshold $c^* \simeq l_B^2/k^4a^5N^2$, and for the mesh size, $\xi_m \simeq l_B^{1/3}/k^{2/3}a^{5/6}c^{1/2}$. It was indeed observed for a corresponding experimental system that $\xi_m \propto c^{-1/2}f^0$, the f^0 dependence suggests counterion condensation.[37,38] Furthermore, it was shown for the same system[38] that the osmotic pressure (that is governed by the presence of free counterions) is independent of f, clearly indicating the phenomenon of counterion condensation. Using $\xi_m \simeq k^{4/3}a^{5/3}g_m/l_B^{2/3}$ (cf. eq 4) we arrive at

$$L \simeq \frac{k^{1/3}a^{5/12}N^{1/2}}{c^{1/4}l_B^{1/6}} \tag{17}$$

The chains shrink with decreasing l_B^{-1}, $L \propto l_B^{-1/6}$, and at $l_B^{-1} \simeq 1/k^2a^{5/2}c^{1/2}N$ one enters the dilute regime 8.

Poor Solvent, Overlapping Chains without Condensed Counterions (Regime 6_o in Figure 3). At high temperatures the chains do not overlap (regime 3 and 6 in Figure 3). At $l_B^{-1} \simeq f^2b^5c^{1/2}N/|v|^{3/2}$ one has $c = c^*$ where c^* is given by $c^* \simeq |v|^3/f^4b^{10}l_B^2N^2$ (using eq 5 for L). Then, in regime 6_o the mesh size is given by $\xi_m \simeq |v|^{1/2}/f^{2/3}c^{1/2}b^{5/3}l_B^{1/3}$ and the chain size obeys[36]

$$L \simeq \frac{f^{1/3}b^{5/6}l_B^{1/6}N^{1/2}}{|v|^{1/4}c^{1/4}} \tag{18}$$

For smaller values of l_B^{-1}, we cross into the regime where the short-range attraction between the monomers can be neglected, i.e., where $\xi_{el} < \xi_T$ (regimes 4_o and 7_o in Figure 3).

Poor Solvent, Collapsed Chains with Condensed Counterions (Regime 9 in Figure 3). For smaller values of l_B^{-1}, the chains collapse in a first-order type fashion into a collapsed state with $L \simeq b^2N^{1/3}/|v|^{1/3}$. Corresponding experiments with salt-free PSS-solutions[37,39] are, up to now, not well understood for three reasons: (i) The osmotic pressure Π shows a strong f dependence (Π increases roughly linearly with f). (ii) The position of the characteristic peak q^* scales roughly

as $f^{0.9}$. (iii) q^* gradually changes from a $c^{1/2}$ to a $c^{1/3}$ dependence when f is decreased. Since in all these systems counterion condensation is expected, these observations may indicate aggregation of chains. With decreasing f, the number of ionic groups per chain goes down so that the effective hydrophobicity of the chain increases, resulting in larger aggregates with more condensed counterions per chain. The average distance between aggregates may show a $c^{-1/3}$ dependence that is reflected in the position of the characteristic peak.

Finally, a similar scenario is expected for Θ and good solvents at sufficiently low temperatures, cf. line A and B in Figure 3.

Semidilute Solutions at Higher Ionic Strength. We give here a few short remarks on the most involved case of a semidilute solution of polyelectrolytes with added salt. In this case one has to keep track of six different length scales: the blob size ξ_T induced by the short-range interaction between the monomers, the electrostatic blob size ξ_{el}, the mesh size ξ_m of the network, the screening length κ^{-1}, the electrostatic persistence length l_e, and the total size L of the chain. As a consequence the complete phase diagram for this situation is quite involved. For low ionic strenth so that the screening length is larger than the mesh size, i.e., $\kappa^{-1} > \xi_m$, one has still the situation discussed above: A given chain forms a straight line of electrostatic blobs within each mesh but is deflected when it "crosses" other chains. This leads to a persistence length of the order of the mesh size. However, as soon as $\kappa^{-1} < \xi_m$, the interaction between different chains may be screened since the typical distance between crossing chains is on the order of ξ_m. If one inserts a test chain into this solution, it will only be deflected if it crosses other chains within a distance smaller than κ^{-1}. Using simple geometrical arguments it can be shown that this occurs typically every distance ξ_m^2/κ^{-1} along the chain. This suggests a modified electrostatic persistence length $\tilde{l}_e$ with $\xi_m < \tilde{l}_e \simeq \xi_m^2/\kappa^{-1} < l_e$, a result that was obtained in ref 35 using an energy balance argument. For even higher ionic strength so that $\kappa^{-1} < \xi_m^2/l_e$, the presence of other chains perturbs the electrostatic persistence length, eq 8, only slighly (cf. section VI. C. in ref 3).

V. Conclusion

We have presented a scaling picture for solutions of flexible polyelectrolytes for a wide range of chain concentration and ionic strength. This is an extension of the scaling theory for polyelectrolytes to include charge renormalization. Remarkably, we find that for all ionic strengths and chain concentrations the electrostatic blob size, which determines the effective "contour length" of the chain remains constant. However, the configuration of the chain does depend on c and c_s. At the largest length scales, one finds stretched chains in the dilute salt-free case; at higher ionic strengths the chains assume configurations of self-avoiding walks, and in the case of interpenetrating chains, Gaussian statistics governs the behavior. Depending on the ratios of different length scales (total chain size, thermal length due to short-range attraction/repulsion, electrostatic blob length, electrostatic persistence length, mesh size), one encounters different chain statistics for smaller portions of the chains.

An interesting aspect of these systems is the non-monotonic dependence of the contour length of the chain on temperature. Starting from high tempertures, the chain begins to stretch with decreasing temperature. Then, as soon as counterion condensation sets in, one finds a shrinkage of the chains. In our scaling picture, this effect can be understood as an effect of charge renormalization together with a change of the solvent quality to poorer conditions. For semidilute solutions this leads to the following reentrant behavior: Starting at, e.g., very high temperatures where the chains are not stretched and may form a dilute solution, one enters semidilute conditions at intermediate values of the temperature. Finally, if the temperature is decreased sufficiently, counterion condensation will cause a shrinkage of the chain, and one reenters the dilute case.

Finally, we note that there are several open questions in this problem. A more rigorous approach to the role of the charge fluctuations along the chain (in the case of condensed counterions) is still missing. The behavior of polyelectrolytes in poor solvents needs a closer inspection by means of experiments and computer simulations. Up to now, experimental facts[37,39] and simulations results[6] do not lead to a conclusive picture. In any case we hope that the presented scaling picture may be a guide for further experiments and computer simulations.

Acknowledgment. The author wishes to thank P. Pincus, K. Kremer, W. M. Gelbart, M. Olvera de la Cruz, C. E. Williams, B.-Y. Ha, C. Holm, A. V. Dobrynin, R. Menes, T. B. Liverpool, and M. Deserno for valuable discussions. I acknowledge financial support by NSF Grants No. DMR--9708646 and No. MRL-DMR-9632716.

References and Notes

(1) de Gennes, P. G.; Pincus, P.; Velasco, R. M.; Brochard, F. *J. Phys. (Paris)* **1976**, *37*, 1461.
(2) Pfeuty , P. *J. Phys.* **1978**, *39*, C2−149.
(3) Barrat, J.-L.; Joanny, J.-L. *Adv. Chem. Phys.* **1996**, *94*, 1.
(4) Stevens, M. J.; Kremer, K. *J. Chem. Phys.* **1995**, *103*, 1670.
(5) Winkler, R. G.; Gold, M.; Reineker, P. *Phys. Rev. Lett.* **1998**, *80*, 3731.
(6) Micka, U.; Holm, C.; Kremer, K. *Langmuir* **1999**, *15*, 4033.
(7) Manning, G. S. *Q. Rev. Biophys.* **1978**, *11*, 179.
(8) Schiessel, H.; Pincus, P. *Macromolecules* **1998**, *31*, 7953.
(9) González-Mozuelos, P.; Olvera de la Cruz, M. *J. Chem. Phys.* **1995**, *103*, 3145.
(10) Brilliantov, N. V.; Kuznetsov, D. V.; Klein, R. *Phys. Rev. Lett.* **1998**, *81*, 1433.
(11) Olvera de la Cruz, M.; Belloni, L.; Delsanti, M.; Dalbiez, J. P.; Spalla, O.; Drifford, M. *J. Chem. Phys.* **1995**, *103*, 5781.
(12) Golestanian, R.; Kardar, M.; Liverpool, T. B. *Phys. Rev. Lett.* **1999**, *82*, 4456.
(13) $e^2Z/\epsilon L$ represents the electrostatic interaction between an isotropic chain of size L and a nearby counterion. For the extended chains considered here, one has $L \gg \xi_{el}$. This leads to a logarithmic correction so that the actual value is of the order $(e^2Z/\epsilon L)\ \ln\ (L/\xi_{el})$. Throughout this paper we neglect this logarithmic factor.
(14) Alexander, S.; Chaikin, P. M.; Grant, P.; Morales, G. J.; Pincus, P.; Hone, D. *J. Chem. Phys.* **1984**, *80*, 5776.
(15) Oosawa, F. *Polyelectrolytes*; Dekker: New York, 1971.
(16) de Gennes, P. G. *Scaling Concepts in Polymer Physics*; Cornell University Press: Ithaca, NY, 1979.
(17) Rayleigh, Lord *Philos. Mag.* **1882**, *14*, 184.
(18) Khokhlov, A. R. *J. Phys. A* **1980**, *13*, 979.
(19) Raphael, E.; Joanny, J.-F. *Europhys. Lett.* **1990**, *13*, 623.
(20) Dobrynin, A. V.; Rubinstein, M.; Obukhov, S. P. *Macromolecules* **1996**, *29*, 2974.
(21) In the necklace picture[20] the globule (regime 3) becomes unstable at $l_B^{-1} \simeq f^2b^2N/2|v|$ and splits into two beads connected by a string (dumbbell). Then at $l_B^{-1} \simeq f^2b^2N/N_{bead}|v|$ ($N_{bead} = 3, 4, ...$) one has a cascade of transitions into necklaces with N_{bead} beads. Finally, at $l_B^{-1} \simeq f^2b^8/|v|^3$ the size of the beads is of the same order as the diameter of the strings so that then the cylindrical and the necklace state become identical. At the phase boundary between 7 and 9 the necklace and the cylinder are again identical and, as

discussed above, unstable due to counterion condensation; in fact, this is also found in ref 22 calculating counterion condensation on the necklace. The boundary between phases the 6 and 9 is also identical in both models. For the cylindrical model one finds that counterion condensation sets in when $l_B^{-1} = |v|^3/k^3fb^{10}$. The same value is found in the necklace case when one calculates the onset of counterion condensation on single beads of the necklace.[22]

(22) Dobrynin, A. V.; Rubinstein, M. *Macromolecules* **1999**, *32*, 915.

(23) Holm, C. Private communication.

(24) Odijk, T. *J. Polym. Sci.* **1977**, *15*, 477.

(25) Skolnick, J.; Fixman, M. *Macromolecules* **1977**, *10*, 944.

(26) Consider a rigid chain with bare persistence length l_P and a repulsion between monomers with a range $\kappa^{-1} \ll l_P$ of functional form $g(r)$ (r is the distance between interacting particles). A given monomer interacts with $n \simeq \kappa^{-1}/b$ neighbours. If we slightly bend the rod so that it has a curvature $R^{-1} \ll \kappa$, then due to symmetry n increases by $\Delta n \simeq n\theta^2$ (where the angle θ is given by $\kappa^{-1}/R \simeq 2 \sin \theta \simeq \theta$). Thus by bending the rod we bring in new material within the range of interaction of the given monomer. Thus the energy increases by an amount $\Delta E \simeq (L/b)\Delta n g(\kappa^{-1}) \simeq (\kappa^{-3}L/b^2R^2)$-$g(\kappa^{-1})$ leading to an effectively larger persistence length $l_P + l_e$ with $l_e \simeq (\kappa^{-3}/b^2)g(\kappa^{-1})$. Example: If one has an interaction of the form $g(r) = l_B e^{-\kappa r}/r^{d-2}$ (Debye−Hückel law in d dimensions) we obtain $l_e \simeq l_B/b^2\kappa^{d-5}$, in agreement with a rigorous perturbation calculation.[27]

(27) Ha, B.-Y.; Thirumalai, D. *J. Phys. II Fr.* **1997**, *7*, 887.

(28) Khokhlov, A. R.; Khachaturian, K. A. *Polymer* **1982**, *23*, 1742.

(29) Li, H.; Witten, T. A. *Macromolecules* **1995**, *28*, 5921.

(30) Ha, B.-Y.; Thirumalai, D. *J. Chem. Phys.* **1999**, 7533.

(31) Netz, R. R.; Orland, H. *Eur. Phys. J. B* **1999**, *8*, 81.

(32) Micka, U.; Kremer, K. *Europhys. Lett.* **1997**, *38*, 279. Micka, U.; Kremer, K. *Phys. Rev. E* **1996**, *54*, 2653.

(33) Odijk, T.; Houwaart, A. C. *J. Polym. Sci.* **1978**, *16*, 627.

(34) Stevens, M. J.; Plimpton, S. J. *Eur. Phys. J. B* **1998**, *2*, 341.

(35) Witten, T. A.; Pincus, P. *Europhys. Lett.* **1987**, *3*, 315.

(36) Dobrynin, A. V.; Colby, R. H.; Rubinstein, M. *Macromolecules* **1995**, *2*, 1859.

(37) Essafi, W.; Lafuma, F.; Williams, C. E. *J. Phys. II Fr.* **1995**, *5*, 1269.

(38) Essafi, W.; Lafuma, F.; Williams, *Eur. Phys. J. B* **1999**, *9*, 261.

(39) Williams, C. E. Private communication.

MA990051K